SOUTH AFRICAN ACTUARIAL JOURNAL
SAAJ **15** (2015) 1–30
http://dx.doi.org/10.4314/saaj.v15i1.1

A scenario approach to estimate the maximum foreseeable loss for buildings due to an earthquake in Cape Town

By A Kijko, A Smit and N Van De Coolwijk

Submission received 11 July 2014
Accepted for publication 28 January 2015

ABSTRACT

A methodology for the assessment of the probable maximum loss associated with an earthquake is described and applied to the Cape Town central business district. The calculations are based on the effect of the two largest earthquakes that occurred in Milnerton in 1809 and Ceres–Tulbagh in 1969. The investigation concludes that if buildings and infrastructure in an area follow the SANS Standard 10160 for seismic loading of 0.1 g, they are exposed to significant seismic risk. The main purpose of this research is not the accurate quantification of expected losses to Cape Town's infrastructure, but to raise awareness between civil engineers, the insurance industry and disaster management agencies that seismic hazard is an issue in South Africa and must be considered as a potential threat to its residents and infrastructure.

KEYWORDS

Probable maximum loss (PML); seismic risk; hazard; expected damage; Cape Town; short-term insurance

CONTACT DETAILS

Prof Andrzej Kijko, University of Pretoria Natural Hazard Centre Africa, University of Pretoria, Private Bag X20, Hatfield, Pretoria 0028; Tel: +27(0)12 420 3613; Email: andrzej.kijko@up.ac.za
Ansie Smit, University of Pretoria Natural Hazard Centre Africa, University of Pretoria, Private Bag X20, Hatfield, Pretoria 0028; Tel: +27(0)12 420 2282; Email: ansie.smit@up.ac.za
Natalie Van De Coolwijk, Willis Re (Pty) Ltd, First Floor, Building 3, Inanda Greens Office Park, 54 Wierda Road West, Wierda Valley, 2196; Tel +27(0)11 082 3803
Email: Natalie.vandecoolwijk@willis.com

1. INTRODUCTION

1.1 Seismic risk estimation involves the assessment of the adverse consequences that a society may be subjected to as a result of future earthquakes. This includes the estimation of the probability of the occurrence of observed consequences. Such estimation is of paramount importance to disaster management centres, and the insurance and reinsurance industry, especially concerning heavily populated areas that are subjected to natural or induced seismic activity. A tool is therefore needed to investigate the damage and losses that may be incurred as a result of an earthquake.

1.2 Comprehensive reviews of seismic risk and loss estimation methodologies developed and used in the United States of America (USA) up to the 1980s have been compiled by Reitherman (1985) and Whitman (1986). Equivalent studies have been performed in the former Soviet Union and were applied in the assessment of earthquake losses for the largest cities of the world (Keilis-Borok, Kronrod & Molchan, 1984). More recent reviews of work done in Russia can be found in Frolova, Larinov & Bonnin (2006) and Sobolev (1997). The National Institute of Building Sciences (NIBS) under the Federal Emergency Management Agency (FEMA), both in the USA, conducted an excellent review of the state-of-the-art earthquake loss estimation methodologies, including the HAZUS methodology. The review 'Assessment of the State-of-the-Art Earthquake Loss Estimation Methodologies' (FEMA-249, 1994), which covers all aspects of the problem of earthquake loss estimation, is probably the most comprehensive ever written on this subject.

1.3 The questions that are asked persistently by the South African public, media, disaster management centres and the insurance industry alike are whether or not Cape Town's citizens and infrastructure are at risk of a strong seismic event and, if so, how big the threat is? Deterministic seismic hazard (DSHA) and risk (DSRA) analyses are used to answer this question in an understandable manner. The occurrence of three possible but hypothetical seismic events in and near Cape Town are investigated. One disadvantage faced during this investigation was the lack of available data in South Africa needed for reliable quantification, making seismic hazard and risk assessment in the country exceedingly difficult. This paper therefore only provides a first approximation of South Africa's expected seismic hazard and risk.

1.4 The study concentrates only on deterministic seismic hazard and risk assessments, complementing the work by Davies & Kijko (2003), where hazard and risk assessment are presented from the probabilistic point of view. Section 2 provides a description of the applied seismic risk estimation procedure; definitions and assumptions are provided in Section 3. A discussion on the appropriate ground motion variables to use and an assessment of the maximum regional earthquake magnitude are provided in Sections 4 and 5 respectively. Section 6 provides the application of the theory, as defined in the previous sections, to three plausible earthquake scenarios for Cape Town.

2. BACKGROUND

2.1 Current seismic risk estimation consists of two categories, namely deterministic and probabilistic (Kramer, 1996; Kijko, 2011). These procedures are two sides of the same coin. Combined, the two methodologies provide a complete picture of the earthquake threat that neither of the individual procedures is capable of giving alone (Davies & Kijko, op. cit.; McGuire, 2004).

2.2 Typical DSRA starts from a hypothetical, user-defined chosen earthquake, often known as the 'worst case scenario'. The selected earthquake is the largest possible area-characteristic, maximum possible magnitude and is located at the minimum possible distance from the site for which seismic hazard is calculated. With the help of the appropriate attenuation relation, a respectable ground motion parameter is then computed for the site. Finally, the expected damage[1] arising from these ground motions is calculated. This approach is often used in the insurance industry and is useful when a clear strategy is required to manage potential catastrophic losses. The strongest point of the 'scenario earthquake' approach is that it provides a tool for the quantification of an extraordinary earthquake in both size and location and consequently an unusual set of damage and losses.

2.3 For the purpose of this study, deterministic risk analysis is referred to as the probable maximum loss (PML) procedure. The use of the term is incorrect and misleading since the applied methodology does not provide any assessment of probability associated with the calculated loss. Further clarification was sought from Lebek (unpublished)

> The Probable Maximum Loss is a term used in the insurance and reinsurance industry as well as in the Real Estate, for seismic risk assessment. Most seismic PML's are conducted by structural engineers and include on-site inspection and/or building plan review. In the area of Commercial Real Estate due diligence, seismic PML's are often performed according to the scope published by the American Society of Testing Materials Standard E (ASTM E2557-07). Although the definition is not consistent in the insurance industry, it is often generally defined as the anticipated value of the largest loss that could result from the destruction and the loss of use of property. The term PML is one of the most widely used terms in property insurance underwriting. But it represents one of the least clear concepts in all insurance. This fact is reflected by the result of a four-year study that involved collecting the personal and company definitions of PML from over a hundred underwriters and underwriting executives. No two of their definitions fully agree.

In this study the term 'PML' refers to the estimation of the largest loss that could result from the destruction and loss of use of property due to an earthquake.

1 Expected losses are calculated by multiplying the expected damage with the monetary cost of the infrastructure.

2.4 Earthquake magnitudes in this paper are defined in terms of local, M_L Richter scale (Lay & Wallace, 1995). These magnitudes are measured in terms of Richter magnitude which measures how the size of the earthquake relates to the total strain of energy released at the hypocentre of the event. The hypocentre is defined as the point of origin of an earthquake within the earth, compared to the epicentre which is the point on the surface of the earth directly above the hypocentre (Lay & Wallace, op. cit.). The increase of earthquake magnitude by one unit corresponds to the increase in energy released by an earthquake by approximately 30 times. The area-characteristic, maximum possible earthquake magnitude $m_{\max}$ is defined as the upper limit of earthquake magnitude for a given region (EERI Committee, 1984). This parameter is of paramount importance in the methodology for a single earthquake-based PML estimation and accurate knowledge of $m_{\max}$ is therefore crucial. A small difference in the $m_{\max}$ value will cause a significant under- or over-estimation of the resulting damage. Subsequently the best technique for assessment of this parameter is discussed in Section 4. The threshold of completeness ($m_{\min}$) is the lower limit magnitude above which it is assumed that all the seismic events were recorded. This level may change over time. The strength of a seismic event at a given site is measured in terms of the Modified Mercalli Intensity (MMI) scale, a subjective scale based on resultant structural damage to buildings. The MMI felt at a specific location varies according to the distance from the hypocentre of the earthquake to the location (ABS Consulting, Property Risk Glossary).

2.5 Although this study focuses only on the deterministic side of seismic hazard analysis, a full probabilistic seismic hazard analysis can be achieved when, in addition to the damage distributions, probabilities can be assigned to the scenario earthquake as well as to all other possible scenario earthquakes. A probabilistic risk analysis evaluates the probability for all degrees of damage arising from seismic events, including the event considered in the PML procedure. However, the strict classification of seismic risk models into deterministic and probabilistic categories can be misleading. Often the deterministic risk models contain random variables or various probabilistic elements. Early techniques used in earthquake risk assessment employed such models, which included a significant number of statistical elements, in order to estimate the uncertainty of an expected loss from a credible maximum magnitude earthquake. These estimates are deterministic since they are based on an arbitrary set of 'scenario earthquakes' but they make use of statistical tools in providing a distribution for the expected damage as seen in the complementing work by Davies & Kijko (op. cit.).

3. DEFINITIONS AND ASSUMPTIONS

3.1 The DSRA methodology involves the development of a particular seismic scenario, according to which expected damage is calculated. The scenario consists of the assumed occurrence of an earthquake of a specified size and location. A typical DSRA procedure consists of the following five steps:

– Identification and characterisation of all earthquake sources capable of producing significant ground motion at the site.

– Selection of a shortest source-to-site distance. This distance may be expressed as an epicentral or hypocentral distance, depending on the type of the distance used in the attenuation relation of the ground motion. Conventionally, at least in the insurance industry, the effect of the ground motion at a given site is expressed in terms of the MMI scale which is a subjective scale based on resultant structural damage to buildings (Wood & Neumann, 1931).
– Selection of the control earthquake expected to produce the strongest level of shaking. The control earthquake is described in terms of its size and distance from the site. Magnitude size is usually expressed as Richter earthquake magnitude or MMI at the epicentre.
– Calculation of the expected ground motion at the site as generated by the control earthquake.
– Calculation of the expected damage at the site that resulted from these ground motions.

3.2 The DSRA methodology provides a framework for evaluation of the worst-case scenario. However, it provides no information on the likelihood of the occurrence of such a scenario. As in the case of DSHA, DSRA involves subjective assumptions, particularly in regard to earthquake potential as described by the maximum possible earthquake magnitude $m_{\max}$ (Reiter, 1990).

3.3 There are two common assumptions made in the modelling of earthquake occurrence. Firstly, the number of main seismic events in the time interval T follows a Poisson distribution with parameter λT, where λ is the frequency (annual mean activity rate) of earthquake occurrence. Secondly, the earthquake magnitudes follow the Gutenberg–Richter relation (Gutenberg & Richter, 1944),

$$\ln(n) = a - bm \tag{1}$$

where n is the number of earthquakes, m is the earthquake magnitude, a is a constant measuring the level of seismicity and b is a constant which characterises the ratio between small events and large ones. The Gutenberg–Richter relation is the logarithm-frequency-magnitude relation where the plot of the logarithm of the number of earthquakes against the magnitude is linear.

3.4 If the magnitudes of seismic events are assumed to be independent, identically distributed (iid) random variables, the frequency-magnitude Gutenberg–Richter relation (1) can be expressed (Page, 1968) in terms of distribution functions

$$f_M(m) = \begin{cases} 0 & m < m_{\min} \\ \dfrac{\beta \exp\left[-\beta\left(m - m_{\min}\right)\right]}{1 - \exp\left[-\beta\left(m_{\max} - m_{\min}\right)\right]} & m_{\min} \le m \le m_{\max} \\ 0 & m > m_{\max} \end{cases} \tag{2}$$

and

$$F\ (m) = \begin{cases} \dfrac{1-\exp\left[-\ (m-m_{\min})\right]}{1-\exp\left[-\ (m_{\max}-m_{\min})\right]} & \begin{matrix} m & m_{\min} \\ m_{\min} \le m \le m_{\max}, \\ m & m_{\max} \end{matrix} \end{cases} \tag{3}$$

where $f_M(m)$ and $F_M(m)$ are respectively the probability density function (PDF) and cumulative distribution function (CDF) of magnitude m, where $m_{\min} \le m \le m_{\max}$, $\beta = b\ln(10)$ and b is the b-parameter of the Gutenberg–Richter relation (1). The maximum likelihood estimator of the β-value, denoted as $\hat{\beta}$, can be obtained (Page, op. cit.) from the solution of equation

$$\frac{1}{\beta} = \overline{m} - m_{\min} + \frac{(m_{\max}-m_{\min})\exp\left[-\beta(m_{\max}-m_{\min})\right]}{1-\exp\left[-\beta(m_{\max}-m_{\min})\right]}, \tag{4}$$

where $\overline{m}$ is the sample mean magnitude. The value of $\hat{\beta}$ can be obtained only by recursive solutions. The approximate standard error (Aki, 1965) of $\hat{\beta}$, denoted as $\hat{\sigma}_{\beta}$, is

$$\hat{\sigma}_{\beta} = \frac{\hat{\beta}}{\sqrt{n}} \tag{5}$$

such that n is number of earthquakes with magnitudes greater or equal to $m_{\min}$.

3.5 It is also assumed that n earthquakes with magnitudes larger or equal to $m_{\min}$ that occurred in a specified time interval T are recorded. The time span T for the seismic event catalogue is measured in years. The earthquake magnitudes are assumed to be iid random variables with the PDF $f_M(m)$ and CDF $F_M(m)$. The magnitudes are denoted as $m_i\ (i = 1,2,\ldots,n)$ and ordered such that m_n is the maximum observed earthquake and $m_{\min} \le m_1 \le \ldots \le m_n = m_{\max}^{obs} \le m_{\max}$.

3.6 Traditionally in the insurance industry the strength of a seismic event at a given site is expressed in terms of MMI. Connection of the expected MMI at the site to the respective damage and loss distributions are provided by the damage probability matrices (DPM), (Whitman, Reed & Hong, 1973). The extent of damage, ranging from none to total, is divided into damage states, each of which is described both by words and by a range of damage factors. The damage factor denotes the ratio of the value of the physical damage or 'Rand loss', attributable to the earthquake, to the replacement value (ATC-13, 1985). For each MMI of ground shaking, the numbers in the corresponding column provide the distribution of the expected damage. Note that the values in each column sum to 100%. Damage probability matrices for the building classes discussed in this study are available in Appendix A.

3.7 The vulnerability curve, calculated per building class, is the average level of damage per level of intensity. From a statistical point of view, the curve is represented by the function

$$\mathrm{E}\left[D|i\right] = \int_0^{d_{max}} df_D\left(d|i\right)\mathrm{d}d, \tag{6}$$

where $\mathrm{E}\left[\bullet\right]$ denotes the operator of expectancy. The function $\mathrm{E}[D\,|\,i]$ denotes the mean damage factor for a given MMI i (ATC-13, op. cit.). When the function $\mathrm{E}\left[D|i\right]$ is plotted against the ground shaking intensity i, the plot is called the vulnerability curve. In this paper we use the vulnerability curves provided by ATC-13 (op. cit.), in which the conditional PDF $f_D\left(d|i\right)$ is given in the form of Whitman's damage probability matrices DPM_{ij} for seven damage states j (j=1,2,…,7) and nine intensity levels i (i=*IV*,…,*XII*). In ATC-13 (op. cit.), the damage states are called the central damage factors, CDF_j and are defined as:

- no damage when CDF_1 = 0%;
- slight damage when CDF_2 = 0,5%;
- light damage when CDF_3 = 5%;
- moderate damage when CDF_4 = 20%;
- heavy damage when CDF_5 = 45%;
- major damage when CDF_6 = 80%; and
- total destruction when CDF_7 = 100%.

The vulnerability curves can therefore be calculated from equation (6), where the integration is replaced by the summation

$$\mathrm{E}\left[D|i\right] = \sum_{j=1}^{7} CDF_j.DPM_{ij}, \tag{7}$$

and the expected rand loss, for the structure experiencing an MMI, is then calculated as

$$\text{Rand Loss}\left[i\right] = \text{Rand Value of Building} \times \sum_{j=1}^{7} CDF_j.DPM_{ij}. \tag{8}$$

3.8 An integral part of any DSRA is the selection of an area-characteristic ground motion prediction equation (GMPE) and the calculation of the expected ground motion at the site as generated by the control earthquake. An MMI GMPE is a relationship that translates the maximum (focal) MMI at the epicentre (I_0) into MMI at the site. The most often used MMI GMPE relation has the following general form

$$I_0 - I = -a_1 - a_2 \ln r - a_3 r, \tag{9}$$

where a_1,a_2,a_3 are coefficients, r is the chosen epicentral or hypocentral distance in kilometres, I is MMI at the site and I_0 is the maximum (focal) MMI at the epicentre. The numerical values of coefficients a_1,a_2,a_3 are different for different regions and are usually estimated from MMI distribution maps of the region. The empirical relation between earthquake magnitude m and MMI at the epicentre I_0, is given by Richter (1958):

$$I_0 = \frac{3}{2}m - 1. \tag{10}$$

The MMI GMPE for the selected area in this study is (Hattingh, Bejaichund & Ramperthap, 2006) of the form

$$I_0 - I = -2,9829 + 1,2032\ln(r) + 0,0010073\,r\,, \tag{11}$$

where the standard deviation of the above conversion is of the order of three-quarters of an MMI unit.

4. SELECTION OF GMPE: MMI vs PGA

4.1 The selection of an appropriate GMPE is crucial in any quantification of seismic hazard and therefore risk (e.g. Budnitz et al., 1997; McGuire, 2004). However, GMPEs expressed in terms of Peak Ground Acceleration (PGA) and/or spectral acceleration for South Africa could not be found in the available literature. At least two reasons exist why GMPEs have not been developed for South Africa. The first is that, because of the low levels of natural seismicity in South Africa, there is not enough information to construct reliable GMPEs. Secondly, South Africa has never had an extensive network of local accelerometers needed to construct local PGA-based GMPEs.

4.2 One of the suggestions was for South Africa to make use of Next Generation Attenuations (NGAs) as prepared by the Pacific Earthquake Engineering Research Group (PEER). This suggestion seems appealing but it should be kept in mind that of the 3551 strong ground motion records used in the construction of the NGAs none of them was observed in Africa (Chiou et al., 2008).

4.3 This problem was extensively discussed during the Senior Seismic Hazard Analysis Committee (SSHAC) Level 3 Close-out Workshop, held during October 2013 in Pretoria, South Africa. This committee was established to analyse the seismic hazard assessment for Thyspunt, a potential location of a future nuclear power plant in South Africa. During the workshop several alternative approaches to construct a South African characteristic GMPE were presented (Bommer et al., 2013; Rietbrock, unpublished; Rietbrock, Strasser & Edwards, 2013; Scherbaum, unpublished). Summarising these attempts to construct GMPEs for South Africa led to the conclusion that the best GMPEs for South Africa can be obtained through synthetic modelling and/or adoption of GMPEs from tectonically similar regions. An alternative solution to utilise a comprehensive collection of macroseismic records was proposed by Hattingh, Bejaichund & Ramperthap (op. cit.) and Midzi et al. (2013). These records date back to 1932 and consist of more than 40 isoseismal maps of the strongest natural and mine-related events. Based on these MMI records, MMI GMPEs characteristic for different South African areas were developed. Most attempts to quantify seismic hazard and risk in South Africa, including this study, make use of the GMPE in terms of MMI.

4.4 Despite the fact that the concept of MMI is at least 80 years old, it is still the subject of extensive research all around the world. The MMI scale and MMI-based GMPEs are the focus of continuous investigations in the USA (Dengler & Dewey, 1998; Bakun, 2000; Dewey, Wald & Dengler, 2000; Kaka & Atkinson, 2004; Bakun 2006), Canada (Jalpa & Atkinson, 2012) and Central Asia (Bindi et al., 2014). These equations are built into the ShakeMap code (Atkinson & Kaka, 2006) and they are used, for example, in Chile (Barrientos et al., 2004), and Japan (Bakun, 2005), and are considered as a standard in Europe (EMS98, 1998; Bakun & Scotti, 2006). Allen, Wald & Worden (2012) provide an excellent review of the application of the intensity scale in ShakeMaps in active crustal regions.

4.5 There are several important advantages to using MMI-based GMPEs over the GMPEs based on PGA. One is to account for the local conditions (site effect), which is not an easy task when the GMPEs are expressed in terms of PGA (e.g. Chiou et al., op. cit.). However, site effect is accounted for by default in regional MMI GMPEs.

4.6 Another advantage that the use of MMI has over PGA can be seen in the application of the ATC-13 (op. cit.) vulnerability curves. These curves are expressed in terms of MMI where PGA has to be expressed through the use of analogue curves, especially when the curves are used in conjunction with GMPEs which are also based on MMI. The use of MMI-based damage curves allows for the calculation of seismic risk without additional conversions of PGA to MMI or vice versa. If such conversions are required in the risk assessment procedure, at least a dozen different conversion equations exist. These include equations by Neumann (1954), Gutenberg & Richter (1956a, b), Ambraseys (1974), Trifunac & Brady (1975), Murphy & O'Brien (1977), Lomnitz (1973), Saragoni, Crempien & Ayala (1982), Wald et al. (1999) and Silva et al. (2005). However, similar to the GMPE problem, there is no systematic database of damage due to seismicity for infrastructure in South Africa. The required region-characteristic vulnerability curves needed for risk assessment do not exist. There is little likelihood of obtaining the required information to construct such curves in the near future. These conditions also disqualify the conversion equations by Neumann and others mentioned above since the required calibration data for South African conditions do not exist. This necessitated the use of the ATC-13 (op. cit.) damage curves. Alternative vulnerability curves e.g. Risk-UE (Mouroux et al., 2004) were excluded due to significant uncertainties associated with predicted damage (Goran Trendafiloski,[2] personal communication, 2011).

4.7 Our assessments of hazard and risk are based on the application of regional GMPE in terms of MMI. However, for the purpose of verification of our results, we performed several additional calculations in terms of PGA—the maximum acceleration amplitude measured (or expected) of an earthquake. Since there is no single GMPE in terms of PGA characteristic to South Africa we applied five different PGA-based attenuations which were developed for areas with a geological environment similar to a large extent to that of South Africa.

2 Goran Trendafiloski, Impact Forecasting, Aon Benfield, United Kingdom

Two GMPEs (Jonathan, 1996; Twesigomwe, 1997) were derived for Africa and GMPEs by Toro, Abrahamson & Schneider (1997) and Atkinson & Boore (2006) are derived for stable continental areas. The NGA GMPEs by Boore & Atkinson (2008) are perhaps the least applicable set of equations to South Africa since not one observed strong motion record on the African continent was taken into consideration during their development. Tables 1 and 2 provide the expected PGA at the Green Point Stadium as generated by earthquakes of magnitude 6,30 and 6,96 located at the Milnerton fault.

TABLE 1. Expected values of PGA at the site of Green Point Stadium generated by an earthquake of magnitude 6,30 located at the Milnerton fault as per five different ground motion prediction equations

Ground motion prediction equation	Predicted PGA at Green Point Stadium (g)
Atkinson & Boore (2006)	0,32
Toro, Abrahamson & Schneider (1997)	0,29
Jonathan (1996)	0,36
Twesigomwe (1997)	0,27
Boore & Atkinson (2008)	0,13

TABLE 2. Expected values of PGA at the site of Green Point Stadium generated by an earthquake of magnitude 6,96 located at the Milnerton fault as per five different ground motion prediction equations

Ground motion prediction equation	Predicted PGA at Green Point Stadium (g)
Atkinson & Boore (2006)	0,49
Toro, Abrahamson & Schneider (1997)	0,50
Jonathan (1996)	0,71
Twesigomwe (1997)	0,47
Boore & Atkinson (2008)	0,19

It is important to note that, in reality, the predicted values of PGA shown in both these tables can be significantly exceeded. The tables show only the median PGA values as estimated for hard rock. If the stadium structure is not situated at the hard rock, the observed values can be significantly larger. All calculations were also performed for a relatively short epicentral distance of approximately 10 kilometres. It is known that, at such short distances, the fluctuations of PGA are significant.

4.8 Despite the large uncertainties associated with PGA assessments the predicted values in Tables 1 and 2 are very conservative. This is because South Africa is situated on a so-called stable continental area which is characterised by the extremely low attenuation of

seismic waves. Therefore even weak seismic events can be felt at large distances and cause damage. Two events should serve as a serious warning against the underestimation of the damaging effect which earthquakes can have in this country. The Mozambique magnitude 7,0 earthquake of 22 February 2006 was felt and caused damage in Durban, approximately 1000 km from its epicentre. The recent, and in absolute terms, a weak, local magnitude 5,4 seismic event in Orkney, 150 kilometres south-west of Johannesburg, on 5 August 2014 caused one death and significant damage to infrastructure. This event was felt across most of South Africa, Mozambique and Botswana. An event of magnitude 5,4 is 250 times weaker, in terms of released energy than the worst case scenario of magnitude 7,0 estimated in Cape Town (Section 5).

5. ASSESSMENT OF THE MAXIMUM REGIONAL EARTHQUAKE MAGNITUDE

5.1 Suppose that in the area of concern, in a specified time interval T, there are n earthquakes with magnitudes $m_1,\ldots,m_n$. Each magnitude $m_i \geq m_{\min}$ $(i=1,\ldots,n)$, where $m_{\min}$ is a known threshold of completeness, are recorded. It is further assumed that the earthquake magnitudes are iid random variables with the PDF $f_M(m)$, and the CDF $F_M(m)$. The variable $m_{\max}$ is the unknown, upper limit of the range of magnitudes and is thus termed the maximum regional earthquake magnitude.

5.2 The random variable m_n, which is the largest observed magnitude (also denoted as $m_{\max}^{obs}$, has a CDF

$$F_M(m) = \begin{cases} 0 & m < m_{\min} \\ \left[F_M(m)\right]^n & m_{\min} \leq m \leq m_{\max}. \\ 1 & m > m_{\max} \end{cases} \tag{12}$$

After integrating by parts, the expected value of M_n, $E(M_n)$, is

$$E(M_n) = \int_{m_{\min}}^{m_{\max}} m\,dF_{M_n}(m) = m_{\max} - \int_{m_{\min}}^{m_{\max}} [F_{M_n}(m)]^n\,dm. \tag{13}$$

Hence

$$m_{\max} = E(M_n) + \int_{m_{\min}}^{m_{\max}} [F_{M_n}(m)]^n\,dm. \tag{14}$$

By replacing the expected value of the largest observed magnitude $E(M_n)$ with the largest magnitude already observed $m_{\max}^{obs}$, equation (14) becomes (Kijko, 2004)

$$m_{\max} = m_{\max}^{obs} + \int_{m_{\min}}^{m_{\max}} [F_{M_n}(m)]^n \, \mathrm{d}m \,, \tag{15}$$

in which the desired $m_{\max}$ appears on both sides. The estimated value of $m_{\max}$ (denoted as $\hat{m}_{\max}$) can therefore be obtained only through iteration. The estimator of $m_{\max}$ becomes a function of the known observations $m_{\max}^{obs}$ and n, and is obtained as a root of equation (15). The above result is valid for any CDF of earthquake magnitude $F_M(m)$.

5.3 Equation (15) is, by its nature, very general and has several interesting properties. For example, it is valid for each PDF, or equivalently $f_M(m)$, and does not require the fulfilment of any additional conditions. It may also be used when the exact number of earthquakes (n) is not known. In this case, the number of earthquakes can be replaced by its expected value λT. Such a replacement is based on the standard assumption in seismology that the number of earthquakes occurring in unit time conforms to a Poisson distribution with parameter λ in the time span T. It is also important to note that, since the correction term

$$\Delta = \int_{m_{\min}}^{m_{\max}} \left[F_M(m) \right]^n \mathrm{d}m, \tag{16}$$

is never negative, equation (15) provides a value of $\hat{m}_{\max}$ which is never less than the largest magnitude already observed.

5.4 Cooke (1979) was probably the first to obtain an estimator of the upper bound of a random variable similar to equation (15). The difference between equation (15) and the original estimator by Cooke (op. cit.) is that the former provides an equation in which the upper limit of the integration is $m_{\max}^{obs}$, not the unknown $m_{\max}$. For large n, when the value of $m_{\max}^{obs}$ and $m_{\max}$ are close to each other, the two solutions are asymptotically equivalent. For the frequency-magnitude Gutenberg–Richter relation (1) with the CDF defined in equation (3), the estimator of $m_{\max}$ requires the calculation of the integral

$$\Delta = \int_{m_{\min}}^{m_{\max}} \left[\frac{1 - \exp\left[-\beta \left(m - m_{\min} \right) \right]}{1 - \exp\left[-\beta \left(m_{\max} - m_{\min} \right) \right]} \right]^n \mathrm{d}m \,. \tag{17}$$

Integral (17) does not have a simple solution, but an approximate estimator of $m_{\max}$ can be obtained through the application of Cramér's approximation. According to Cramér (1961), for large n the value of $\left[F_M(m) \right]^n$ is approximately equal to $\exp\left[-n\left(1 - F_M(m) \right) \right]$. It can be shown that after replacement of $\left[F_M(m) \right]^n$ by its Cramér approximation, the estimator of $m_{\max}$ is obtained (Kijko & Sellevoll, 1989; Kijko, 2004) as an iterative solution of the equation

$$m_{\max} = m_{\max}^{obs} + \frac{E_1(n_2) - E_1(n_1)}{\beta \exp(-n_2)} + m_{\min} \exp(-n), \tag{18}$$

where $n_1 = n / \left\{1 - \exp\left[-\beta\left(m_{\max} - m_{\min}\right)\right]\right\}$, $n_2 = n_1 \exp\left[-\beta\left(m_{\max} - m_{\min}\right)\right]$ and $E_1(\bullet)$ denotes an exponential integral function (Abramowitz & Stegun, 1970). Numerical tests based on simulated data show that when $m_{\max} - m_{\min} \leq 2$ and $n \geq 100$, the parameter $m_{\max}$ in n_1 and n_2 can be replaced by $m_{\max}^{obs}$, thus providing an $m_{\max}$ estimator which can be obtained without iterations. The value of $m_{\max}$ obtained from the solution of (15) is often called the Kijko–Sellevoll (K–S) estimator of $m_{\max}$ (Lasocki & Urban, 2010). The approximate variance of the K–S estimator of $m_{\max}$ for the frequency-magnitude Gutenberg–Richter distribution is of the form

$$\mathrm{VAR}\left(\hat{m}_{\max}\right) = \sigma_M^2 + \left[\frac{E_1(n_2) - E_1(n_1)}{\beta \exp(-n_2)} + m_{\min} \exp(-n)\right]^2, \tag{19}$$

where σ_M denotes standard error in the determination of the largest observed magnitude $m_{\max}^{obs}$.

5.5 A shortcoming of the K–S equation for $m_{\max}$ estimation comes from the implicit assumption that the mean seismic activity rate λ and the *b*-value of the Gutenberg–Richter remain constant in time and that the functional forms of number and magnitude distributions properly describe the observations. Often seismic processes are composed of temporal trends, cycles, oscillations and random fluctuations. When the variation of seismic activity is a random process the Bayesian formalism, in which the model parameters are considered as random variables, provides the most efficient tool in accounting for the uncertainties considered above (e.g. DeGroot, 1970). The rest of the section presents a K–S equation for the assessment of the maximum regional earthquake magnitude in which the uncertainty of the Gutenberg–Richter parameter *b* is taken into account.

5.6 On the assumption that the variation of the *b*-value in the frequency-magnitude Gutenberg–Richter relation may be represented by a Gamma distribution with parameters *p* and *q*, the compound (also known as Bayesian) PDF and CDF of earthquake magnitude takes the form (Campbell, 1982):

$$f_M(m) = \begin{cases} 0 & m < m_{\min} \\ \beta C_\beta \left(\dfrac{p}{p + m - m_{\min}}\right)^{q+1} & m_{\min} \leq m \leq m_{\max} \\ 0 & m > m_{\max} \end{cases}, \tag{20}$$

and

$$F_M(m) = \begin{cases} 0 & m < m_{\min} \\ C_\beta \left[1 - \left(\dfrac{p}{p + m - m_{\min}} \right)^q \right] & m_{\min} \le m \le m_{\max} \\ 1 & m > m_{\max} \end{cases}, \quad (21)$$

where C_β is a normalising coefficient. Parameters p and q can be expressed in terms of the mean and variance of the β-value, where $p = \overline{\beta} / \sigma_\beta^2$ and $q = \left(\overline{\beta} / \sigma_\beta \right)^2$. The symbol $\overline{\beta}$ denotes the known mean value of the parameter β, σ_β is the known standard deviation of β that describes its uncertainty, and C_β is equal to $\left[1 - \left(p / (p + m_{max} - m_{min}) \right)^q \right]^{-1}$.

5.7 Following equation (15), the compound version of the K–S equation (Kijko, 2004) becomes

$$m_{\max} = m_{\max}^{obs} + \frac{\delta^{1/q} \exp\left[n r^q / \left(1 - r^q \right) \right]}{\beta} \left[\Gamma\left(-1/q, \delta r^q \right) - \Gamma\left(-1/q, \delta \right) \right], \quad (22)$$

where $r = p / \left(p + m_{\max} - m_{\min} \right)$, $\delta = n C_\beta$ and $\Gamma(\bullet, \bullet)$ is the Incomplete Gamma Function. The above equation (22) is derived by substituting the CDF of earthquake magnitude (21) into the generic equation (15). It thus allows for the uncertainty in β by assuming that it follows a Gamma distribution, as described in ¶4.8. The value of $m_{\max}$ as obtained from the iterative solution of equation (21) is often called the Kijko–Sellevoll–Bayes (K–S–B) estimator of $m_{\max}$. The approximate variance of the K–S–B estimator of $m_{\max}$ for the frequency-magnitude Gutenberg–Richter distribution is of the form

$$\mathrm{VAR}\left(\hat{m}_{\max} \right) = \sigma_{\mathrm{M}}^2 + \left[\frac{\delta^{1/q} \exp\left[n r^q / \left(1 - r^q \right) \right]}{\beta} \left[\Gamma\left(-1/q, \delta r^q \right) - \Gamma\left(-1/q, \delta \right) \right] \right]^2, \quad (23)$$

where σ_M denotes the standard error in the determination of the largest observed magnitude $m_{\max}^{obs}$.

6. EXAMPLE OF APPLICATION

6.1 Area Investigated

6.1.1 The south-western Cape is considered one of the regions with the highest level of tectonic-origin seismic activity in South Africa. Other seismically active areas include the mining-intensive corridor which extends to the north-western part of the Free State, the south-eastern part of North West province and the south-western section of Gauteng. High levels of seismic hazard are also found in parts of the Free State, Gauteng as well as the eastern parts of the North West province. Low levels of hazard can be seen in the northern part of the KwaZulu-Natal. The level of tectonic activity in the vicinity of the densely populated city of Cape Town, means that the Ceres–Tulbagh area and the Milnerton fault are of prime interest thanks in part to the M_L 6.3 magnitude Ceres earthquake on 29 September 1969 and the M_L

FIGURE 1. The Green Point Stadium located in Green Point between Signal Hill and the Atlantic Ocean. The stadium is also located near the Cape Town city centre and V&A Waterfront, a popular tourist and shopping venue. The stadium has a capacity of approximately 70,000 spectators. (Photo: iStock; © Raphael Christinat)

6,3 magnitude earthquake on 4 December 1809 at the Milnerton Fault. Since the epicentre of the Milnerton earthquake is located very close to the Cape Town central business district (CBD) and the Green Point Stadium (Figure 1), it was chosen for further seismic hazard and risk assessment.

6.1.2 The Milnerton earthquake on 4 December 1809, with a local magnitude M_L 6,3, was one of the largest earthquakes in recorded South African history. Its epicentre is associated with the Milnerton Fault, which is located approximately 10 km from the Cape Town CBD. It is therefore natural to expect that the city of Cape Town might be exposed to potential damage caused by a similar earthquake in future, warranting an investigation into the expected PML.

6.1.3 The Ceres–Tulbagh area is considered one of the regions with the highest level of tectonic-origin seismic activity in South Africa. Tectonic seismic activity is observed in this area with the largest and most destructive recorded earthquake in South African history, the 29 September 1969 event located approximately 100 kilometres from the Cape Town CBD. This event was followed by a long sequence of aftershocks, the most severe of which was on 14 April 1970 with a magnitude M_L of 5,7. The worst structural damage resulting from the earthquake occurred in the northern part of the Tulbagh Valley situated close to the epicentre (Keyser, 1974). Structural impairment also occurred to buildings in the towns of Tulbagh, Wolseley, Ceres and Prince Alfred Hamlet. Damage also occurred in the villages of Saron, Gouda and Hermon, and in the towns of Worcester and Porterville. Slight damage was observed in towns as far away as Stellenbosch. Nine deaths resulted from the earthquake and the damage to buildings in the epicentral area was estimated at US$24 million in 1969. A maximum MMI of VIII was observed during the earthquake in the Tulbagh region.

This corresponds to a ground movement of PGA in the range 0,13 to 0,26 g, with median value 0,22 g, (Kijko, Retief & Graham, 2002).

6.2 Seismic Event Catalogue

6.2.1 Seismic events were selected from a catalogue of earthquakes in South Africa that occurred between 1620 and 2013. The data used in this study were compiled from the following three sources: Brandt et al. (2005), Seismological Bulletins published annually by the Council for Geoscience, Pretoria and catalogues provided by the International Seismological Centre in the United Kingdom.

6.2.2 The seismic event catalogue thus compiled was divided into an incomplete part consisting of historical events and three complete parts, each with a different level of completeness. All the earthquake magnitudes were standardised and expressed in units of local Richter magnitudes M_L. The incomplete part of the catalogue spans the period from 1 January 1751 to 31 December 1970, and contains nine of the largest seismic events that occurred during this period. The magnitudes of these events are estimated from macroseismic events which are very uncertain. It was assumed that for all of these events, the standard error in magnitude determination was 0,3. Events prior to 1 January 1751 were not used in the calculations, since they cannot be considered as a reliable source of information for the area. A detailed investigation into the threshold of completeness of the complete sub-catalogues was carried out—see Table 3. For this study it was also assumed that only earthquakes occurring within a radius of 300 km of the epicentre of the scenario earthquake contribute to the information on the maximum possible earthquake magnitude m_{max} of the area.

TABLE 3. Threshold levels of completeness for the South African seismic event sub-catalogues

Year	Magnitude (M_w)	Magnitude standard error
01-01-1971 to 31-12-1990	3,8	0,3
01-01-1991 to 12-31-1995	3,5	0,2
01-01-1996 to 12-31-2013	3,0	0,1

6.3 Building Class Types

6.3.1 Three selected types of buildings as defined in ATC-13 (op. cit.) represent the most typical urban structures found in South Africa and are defined as

- unreinforced masonry, with load bearing wall, low rise (Class #3);
- reinforced concrete shear wall without moment resisting frame, medium rise (Class #8); and
- reinforced concrete shear wall without moment resisting frame, high rise (Class #9).

According to a rough assessment (Davies & Kijko, op. cit.) these types represent more than 70% of all South African urban structures. Figures 2 to 4 are examples of typical buildings of each selected class.

FIGURE 2. Typical example of building class #3 consisting of 'unreinforced masonry, with load bearing wall, low rise'. Source: EMS98 (op. cit.)

FIGURE 3 (above left). Typical example of building class #8 consisting of 'reinforced concrete shear wall, without moment resisting frame, medium rise'. Source: EMS98 (op. cit.)
FIGURE 4 (above right). Typical example of building class #9 consisting of 'reinforced concrete shear, wall without moment resisting frame, high rise'. Source: EMS98 (op. cit.)

6.3.2 Following consultations with two structural engineers, Derek Lee[3] and Professor Jari Puttonen[4] (personal communication, 2014) it was concluded that structures such as the Green Point stadium do not strictly conform to any of the building classes as stipulated in ATC-13 (op. cit.). However the potential damage to Green Point Stadium can be estimated by looking at both the building class descriptions of

– reinforced concrete shear wall with moment resisting frame, medium rise (Class #6); and
– reinforced concrete shear wall with moment resisting frame, high rise (Class #7).

6.3.3 The Green Point Stadium is one of the most recognisable structures in South Africa and was one of the stadia newly built for the FIFA Football World Cup in 2010. It was designed by GMP Architects in cooperation with Louis Karol, Point Architects and Urban Designers, Cape Town. The article 'Cape Town Stadium: Structural challenges' in *Civil Engineering* (2010, p.53), which provided information on the construction of the stadium, indicates that provision for seismic loading was done during construction in accordance to the SANS Standard 10160-4. The SANS Standard 10160-4 specifies that structures in the vicinity of Cape Town (Zone 1, p.11) must sustain PGA of 0,1 g, which corresponds to a return period 475 years or a 10% probability of exceedance within 50 years. It is however

3 Mr Derek Lee, NSE (Nuclear Structural Engineering), South Africa. http://nucse.com/
4 Professor Jari Puttonen, Professor, Structural Engineering and Building Physics, Department of Civil and Structural Engineering at the Aalto University, Finland

not clear to which building class (SANS Standard 10160, Part 4, Section 6, p.19) the Green Point stadium was assigned, nor what the subsequent calculated seismic load was. We therefore assumed in our assessments that during the design and construction of the Green Point Stadium provision was made for 'standard' seismic loading of 0,1 g as given in SANS Standard 10160-4. The PGA of 0,1 g at the designed stadium is compared with the predicted PGAs at the stadium site (Tables 1 and 2). It is important to note that all the predicted values of PGA exceed the designed PGA of 0,1 g despite the approximate nature of our seismic hazard and risk assessments. Similar concern regarding the significance of seismic hazard risk in South Africa is expressed by the recent study of Haas and Van der Kolf (2014).

6.3.4 It is advised that a more detailed analysis should be done which would include any additional available information. Such an analysis should be completed by a team of experts from different fields including a structural engineer familiar with the detailed seismic design of the stadium.

6.4 PML Assessment for Cape Town

6.4.1 The assessment of the PML for Cape Town consists of calculating the possible earthquake scenarios similar to the observed Milnerton and Ceres–Tulbagh earthquakes of 1809 and 1969. It is assumed that this PML can be generated by a seismic source situated at the same location as the Milnerton earthquake of 4 December 1809, viz., with the approximate epicentre coordinates 34,0°S, 18,4°E, (Brandt et al., op. cit.) and at the Ceres–Tulbagh earthquake location with the approximate epicentre coordinates of 33,28°S and 19,24°E (Green & Bloch, 1971). In both cases it was assumed those hypocentres were located at a depth of 10 km.

6.4.2 It is important to note that there is considerable uncertainty as to the precise location of the Ceres–Tulbagh event. The United States Geological Survey established the epicentre of the event at 32,9°S; 19,7°E. To obtain a more precise location, the records associated with this event were collected from the Pretoria, Grahamstown and Windhoek stations which form part of the World Wide Standard Seismograph Network. For our analyses we utilised the suggested epicentres from Green & Bloch (op. cit.).

6.4.3 The K–S–B procedure in conjunction with the procedure for seismic hazard parameters calculation when data are incomplete and uncertain (Kijko & Sellevoll, 1992) were applied to the input data for both the Milnerton and Ceres–Tulbagh scenarios. The calculated seismic hazard parameters for the two possible earthquake scenarios are provided in Table 4. The results of the hazard analysis in terms of the mean return periods of different magnitudes are given in Figures 5a and b respectively. The mean return period refers here to the average time period between earthquakes with specific characteristics in terms of magnitude and observed area.

6.4.4 The three possible scenarios, based on the Milnerton and Ceres–Tulbagh earthquakes, investigated are

- Milnerton M_L = 6,3, viz. the same magnitude as the event of 4 December 1809;
- Milnerton M_L = 6,96, the worst-case scenario; and
- Ceres–Tulbagh M_L = 7,01, the worst-case scenario.

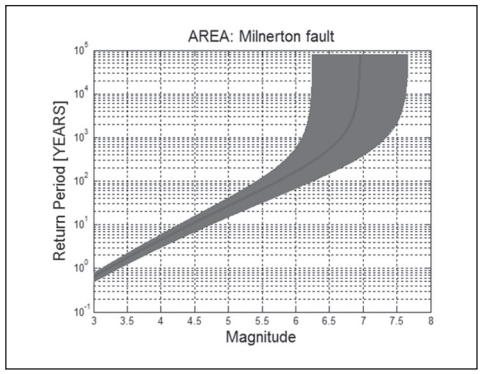

FIGURE 5A. The mean return periods for earthquakes of magnitude between 3,0 and 6,96 for the area in a circle radius of 300 km of the Milnerton fault

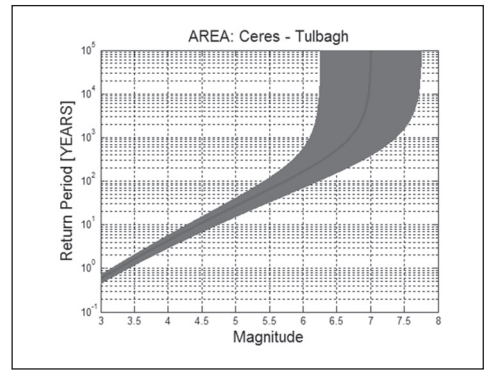

FIGURE 5B. The mean return periods for earthquakes of magnitude between 3,0 and 7,01 units for the area in the circle radius of 300 km with the same epicentre as the 1969 Ceres–Tulbagh earthquake

TABLE 4. Estimated seismic hazard parameters as per the K–S–B and Kijko (2004) procedures

		Milnerton	Ceres–Tulbagh
Level of completeness	$m_{\min}$	≥ 3,0	≥ 3,0
Area-characteristic, maximum possible earthquake magnitude	$\hat{m}_{\max}$	6,96 ± 0,71	7,01 ± 0,75
Gutenberg–Richter parameter	$\hat{b}$	0,90 ± 0,07	0,93 ± 0,07
Mean, annual activity rate	$\hat{\lambda}$	1,59 ± 0,71	1,74 ± 0,40

Based on the assumed magnitudes, the expected damage and its uncertainty intervals were calculated for the three classes of buildings considered, located in the Cape Town centre (classes #3, 7 and 8) as well as the two possible building classes for Green Point Stadium (classes #6 and 7). The results for the three scenarios are listed in Tables 5 and 6. Figures 6 to 8 represent the respective vulnerability curves of the expected damage, in terms of MMI, and its associated uncertainty interval for each of the three scenarios as defined in Table 6.

TABLE 5. Input parameters for seismic risk assessment for the three identified scenarios

	Scenario 1: Milnerton	Scenario 2: Milnerton	Scenario 3: Ceres–Tulbagh
Earthquake magnitude (M_L)	6,3	6,96	7,01
Hypocentral distance	10 km	10 km	~100 km
Predicted MMI	>VIII	>IX	>VII

TABLE 6. Expected damage and uncertainty intervals based on the two Milnerton-fault scenario earthquakes (1 & 2) as well as the Ceres–Tulbagh worst-case scenario earthquake (3)

Building class	Scenario 1		Scenario 2		Scenario 3	
	Expected damage	Uncertainty interval	Expected damage	Uncertainty interval	Expected damage	Uncertainty interval
# 3	30.9%	[18%–44%]	47.6%	[32%–64%]	17.4%	[8%–27%]
# 8	13.2%	[7%–20%]	21.4%	[13%–31%]	7.2%	[3%–12%]
# 9	17.2%	[9%–26%]	28.5%	[18%–40%]	9.5%	[4%–15%]
# 6	9.7%	[4%–15%]	16.7%	[9%–25%]	5.1%	[2%–8%]
# 7	10.8%	[6%–16%]	19.3%	[12%–27%]	5.5%	[2%–9%]

6.4.5 Next, the estimated rand loss is calculated by multiplying the cost of the specified building at the site with the expected damage. Table 7 provides these expected estimates for Green Point Stadium based on the three scenarios as discussed in ¶6.4.4.

TABLE 7. Approximate expected rand loss for the Green Point Stadium, at a building cost of R4,4 billion, for the three scenario earthquakes

	Scenario 1: Milnerton fault event (M_w) (1809)		Scenario 2: Milnerton (worst case)		Scenario 3: Ceres–Tulbagh (worst-case)	
Event magnitude	6,3		6,96		7,01	
Building class	#6	#7	#6	#7	#6	#7
Expected Damages	9.7%	10.8%	16.7%	19.3%	5.1%	5.5%
Expected Rand Loss (million)	R426,8	R475,2	R734,8	R849,2	R224,4	R242

6.5 Potential Impact on Insurance Industry

In an attempt to convert the damage information into actual figures relevant to the insurance industry, let us consider the total value of insured exposures for Cresta Zone 8 (Cape Town), which is estimated to be at least R500 billion. The area covered by the city is 2455 km^2, meaning that these insured structures could reasonably be between 10 km and 50 km from the epicentre of an earthquake. Based on our assumed range of distances from the epicentre and the outcomes of the scenarios outlined above, an overall damage ratio of at least 2% for an earthquake of magnitude M_L 6,3 is plausible. By applying 2% to the total insured value, one obtains an overall loss to the insurance industry from such an earthquake of approximately R10 billion. Due to the very low frequency of natural catastrophes experienced historically in South Africa, the scenarios described are substantially larger events than anything the South African insurance industry has experienced to date. One could speculate that insurance companies would be unprepared to handle a disaster of such magnitude, both in terms of a significant strain on capital reserves as well as the ability to service the resulting claims.

SCENARIO 1 (MILNERTON)

The expected damage and its associated uncertainty for an earthquake of magnitude M_L=6,3 at a hypocentral distance of 10 km for the identified building classes

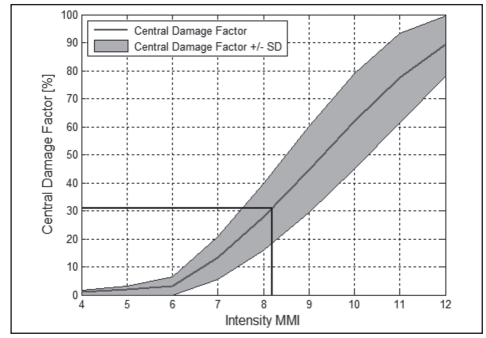

FIGURE 6A. Building Class #3: unreinforced masonry with load bearing wall, low rise building

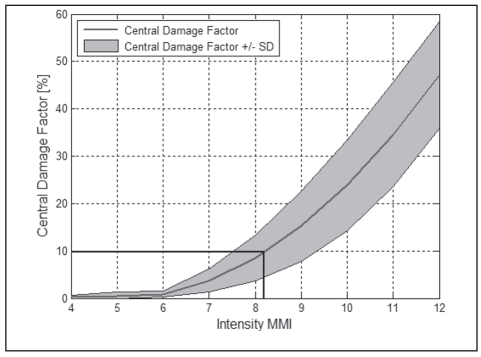

FIGURE 6B. Building Class #8: reinforced concrete shear wall without moment resisting frame, medium rise building

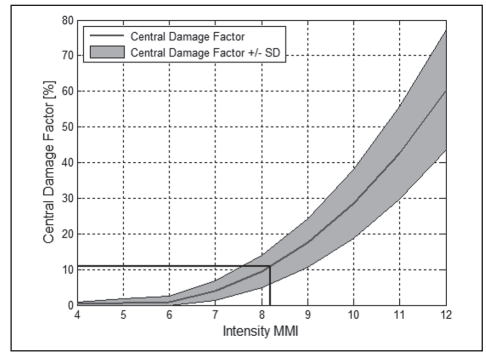

FIGURE 6C. Building Class #9: reinforced concrete shear wall without moment resisting frame, high rise building

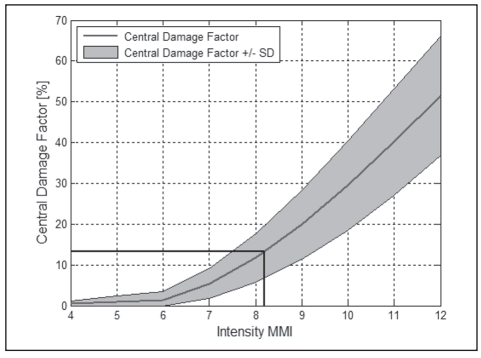

FIGURE 6D. Building Class #6: reinforced concrete shear wall with moment resisting frame, medium rise – Green Point Stadium

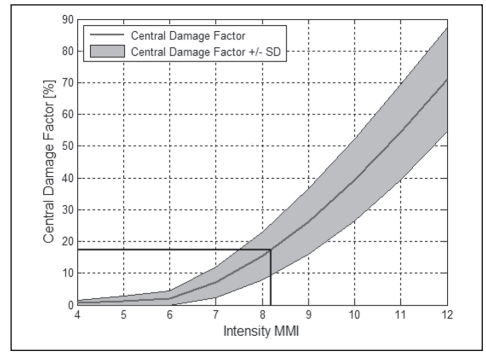

FIGURE 6E. Building Class #7: reinforced concrete shear wall with moment resisting frame, high rise – Green Point Stadium

SCENARIO 2 (MILNERTON)

The expected damage and its associated uncertainty for an earthquake of magnitude M_L=6,96 at a hypocentral distance of 10 km for the identified building classes

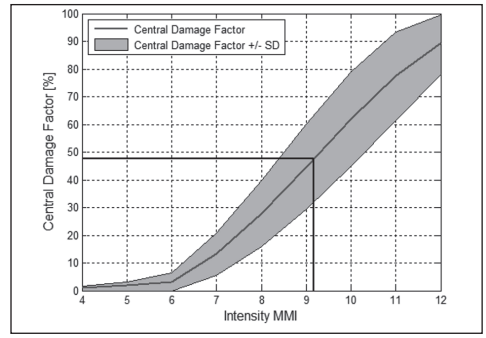

FIGURE 7A. Building Class #3: unreinforced masonry with load bearing wall, low rise building

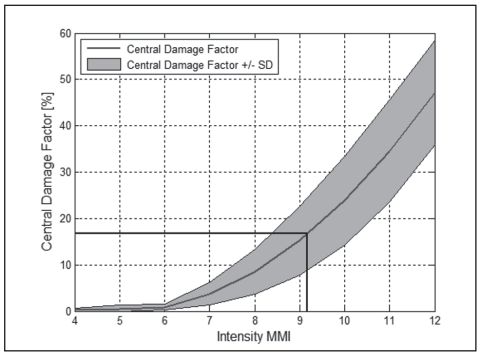

FIGURE 7B. Building Class #8: reinforced concrete shear wall without moment resisting frame, medium rise building

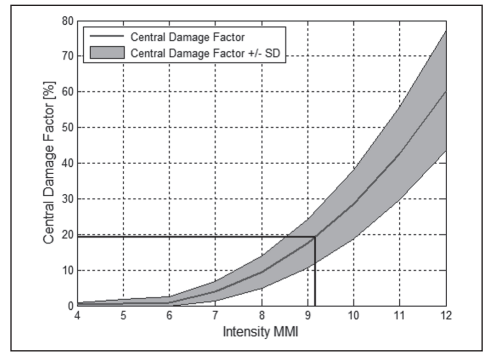

FIGURE 7C. Building Class #9: reinforced concrete shear wall without moment resisting frame, high rise building

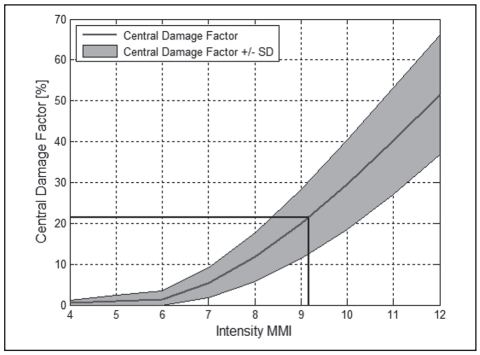

FIGURE 7D. Building Class #6: reinforced concrete shear wall with moment resisting frame, medium rise – Green Point Stadium

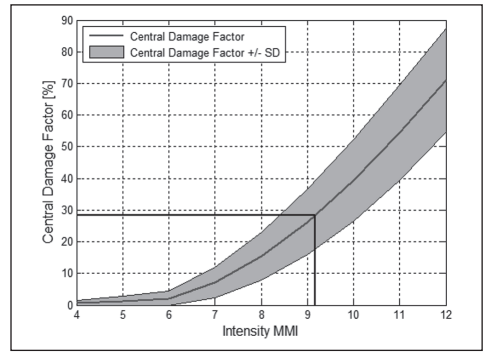

FIGURE 7E. Building Class #7: reinforced concrete shear wall with moment resisting frame, high rise – Green Point Stadium

SCENARIO 3 (CERES–TULBAGH)
Vulnerability curve of the expected damage and uncertainty interval for magnitude M_L=7,01 at a hypocentral distance of 100 km for the identified building classes

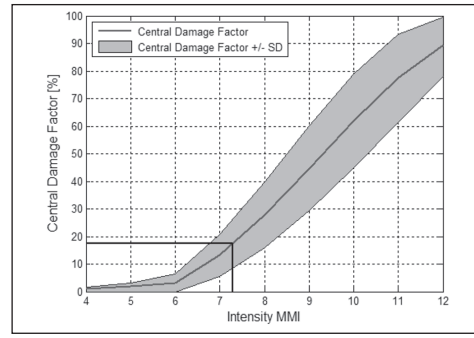

FIGURE 8A. Building Class #3: unreinforced masonry with load bearing wall, low rise building

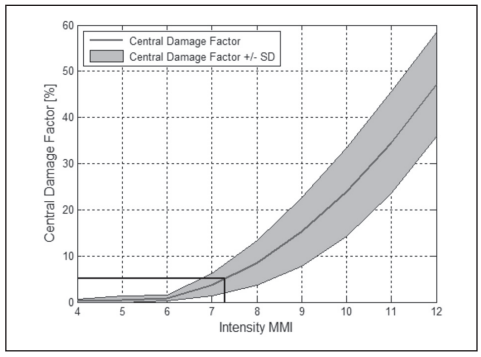

FIGURE 8B. Building Class #8: reinforced concrete shear wall without moment resisting frame, medium rise building

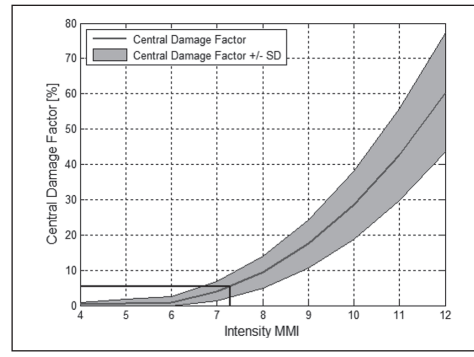

FIGURE 8C. Building Class #9: reinforced concrete shear wall without moment resisting frame, high rise building

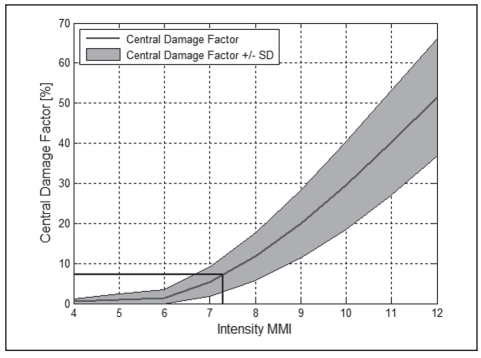

FIGURE 8D. Building Class #6: reinforced concrete shear wall with moment resisting frame, medium rise – Green Point Stadium

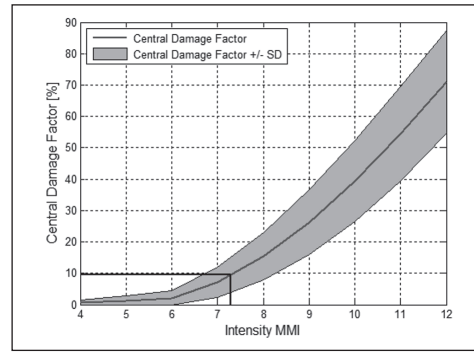

FIGURE 8E. Building Class #7: reinforced concrete shear wall with moment resisting frame, high rise – Green Point Stadium

7. SUMMARY AND CONCLUSION

7.1 The methodology for assessment of the PML from an earthquake has been formulated. This procedure was applied to estimate the approximate expected PML, resulting from three scenario earthquakes, on the three most typical urban structures located in the CBD of Cape Town as well as the Green Point Stadium. For the first two earthquake scenarios it was assumed that the PMLs were generated by an earthquake with magnitudes M_L 6,3 and M_L 6,96. It was assumed that the epicentres of these scenario earthquakes were located at the site of the 1809 Milnerton fault event. For the third earthquake scenario it was assumed that the PML was caused by an event of magnitude M_L = 7,01, located at the epicentre of the 1969 Ceres–Tulbagh event.

7.2 The assessment of the PML applied to the Cape Town CBD proved to be only an approximation because certain information is not readily available. This includes GMPE (Section 4), site effect and seismic loading applied to the Green Point Stadium and other infrastructure (Section 6). To obtain a more accurate assessment of the expected structural loss due to an earthquake, a more detailed analysis is required and should be carried out by a panel of experts in different fields, including a structural engineer familiar with the detailed seismic design of the stadium and infrastructure in Cape Town.

7.3 Despite the approximate nature of our assessments, it is concluded that the seismic risk attributable to a potentially strong earthquake as generated by the Milnerton fault is significant and that the potential seismic risk faced due to occurrence of an earthquake in the Ceres–Tulbagh area is not negligible. The estimated rand loss associated with the predicted damage indicates that significant monetary losses may be incurred by the insurance industry in all three scenarios. Even though the percentage expected damage seems relatively small, the associated monetary loss for all three scenarios can still be substantially larger than has been experienced by the South African market thus far.

7.4 The deterministic methodology applied here may appear simplistic compared to the more preferable probabilistic procedures. However, despite the approximate nature of the results, the three scenarios investigated are sobering. Further analysis on the return period for these large events and the potential for damage due to smaller events is recommended, as well as investigating the risk to an insurer's portfolio.

7.6 The main purpose of our research is to raise awareness among all stakeholders—civil engineers, the insurance industry and disaster management agencies, for example—that seismic hazard is a justifiable concern in South Africa. In particular, seismic hazard in Cape Town must be taken as a serious potential threat to its citizens and to infrastructure. This research provides only an estimated assessment of the seismic hazard and risk (potential losses) to infrastructure due to a strong seismic event in the Cape Town area.

REFERENCES

Abramowitz, M & Stegun, IA (1970). *Handbook of Mathematical Functions*, 9th ed. Dover Publ., New York

ABS Consulting. Property Risk Glossary. http://www.propertyrisk.com/glossary.htm

Aki, K (1965). Maximum likelihood estimate of *b* in the formula log (*N*)=*a*−*bM* and its confidence limits. *Bulletin of the Earthquake Research Institute of Tokyo University* 43, 237–39

Allen, TI, Wald DJ & Worden, CB (2012). Intensity attenuation for active crustal regions. *Journal of Seismology* 16, 409–33

Ambraseys, N (1974). The correlation of Intensity with ground motion, Proc. 14th Conf. Europ. Seism. Comm., Trieste, 1, 335–41. *Bull. Europ. Comm. Earthq. Eng. no. 4*

Applied Technology Council (1985). *ATC-13 Earthquake Damage Evaluation Data for California*, Redwood City, CA

ASTM E2557-07, Standard Practice for Probable Maximum Loss (PML) Evaluations for Earthquake Due-Diligence Assessments, ASTM International, West Conshohocken, PA, 2007, www.astm.org

Atkinson, GM & Boore, DM (2006). Earthquake ground-motion prediction equations for Eastern North America. *Bulletin of the Seismological Society of America* 96, 2181–205

Atkinson, GM & Kaka, SI (2006). Relationships between Felt Intensity and Instrumental Ground Motion for New Madrid ShakeMaps, Report for Award 05HQGR0039, Department of Earth Sciences, Carleton University, Ottawa, QC, Canada, p.27

Bakun, WH (2000). Seismicity of California's north coast. *Bulletin of the Seismological Society of America* 90, 797–812

Bakun, WH (2005). Magnitude and location of historical earthquakes in Japan and implications for the 1855 Ansei Edo earthquake. *Journal of Geophysical Research: Solid Earth* 110 (B2)

Bakun, WH (2006). Estimating locations and magnitudes of earthquakes in Southern California from modified Mercalli intensities. *Bulletin of the Seismological Society of America* 96, 1278–95

Bakun, WH & Scotti, O (2006). Regional intensity attenuation models for France and the estimation of magnitude and location of historical earthquakes. *Geophysical Journal International* 164, 596–610

Barrientos, S, Verae, E, Alvarado, P & Monfret, T (2004). Crustal seismicity in Central Chile. *Journal of South American Earth Sciences* 16, 759–68

Bindi, D, Parolai, S, Gómez-Capera, A, Locati, M, Kalmetyeva, Z & Mikhailova, N (2014). Locations and magnitudes of earthquakes in Central Asia from seismic intensity data. *Journal of Seismology* 18, 1–21

Bommer, JJ, Strasser, FO, Pagani, M & Monelli, D (2013). Quality assurance for logic-tree implementation in probabilistic seismic-hazard analysis for nuclear applications: A practical example, *Seismological Research Letters* 84, 938–45, ISSN: 0895-0695

Boore, DM & Atkinson, GM (2008). Ground-motion prediction equations for the average horizontal component of PGA, PGV, and 5%-damped PSA at spectral periods between 0.01s and 10.0s. *Earthquake Spectra* 24, 99–138

Brandt, MBC, Bejaichund, M, Kgaswane, EM & Roblin, DL (2005). Seismic history of Southern Africa. *Council for Geoscience Seismologic Series* 37*,* ISBN 1-919908-63-3

Budnitz, RJ, Apostolakis, G, Boore, DM, Cluff, LS, Coppersmith, KJ, Cornell, CA & Morris, PA (1997). Recommendations for Probabilistic Seismic Hazard Analysis: Guidance on Uncertainty

and Use of Experts. NUREG/CR-6372, UCR-ID-122160, Main Report 1. Prepared for Lawrence Livermore National Laboratory

Campbell, KW (1982). Bayesian analysis of extreme earthquake occurrences. Part I. Probabilistic hazard model. *Bulletin of the Seismological Society of America* 72, 1689–705

Chiou, B, Darragh, R, Gregor, N & Silva, W (2008). NGA Project Strong-Motion Database. *Earthquake Spectra* 24, 23–44

Civil Engineering (2010). Cape Town Stadium: Structural Challenges, December 2010

Cooke, P (1979). Statistical inference for bounds of random variables. *Biometrika* 66, 367–74

Cramér, H (1961). *Mathematical Methods of Statistics*. Princeton University Press. Princeton

Davies, N & Kijko, A (2003). Seismic risk assessment: with an application to the South African insurance industry. *South African Actuarial Journal* 3, 1–28

DeGroot, MH (1970). *Optimal Statistical Decisions*. McGraw-Hill, New York

Dengler, LA & Dewey, JW (1998). An intensity survey of households affected by the Northridge, California, earthquake of 17 January, 1994. *Bulletin of the Seismological Society of America* 88, 441–62

Dewey, J, Wald, D & Dengler, L (2000). Relating conventional USGS Modified-Mercalli Intensities to intensities assigned with data collected via the Internet. *Seismological Research Letters* 71, 264

European Macroseismic Scale (1998). Grünthal, G. (ed.) (1998), *Cahiers du Centre Européen de Géodynamique et de Séismologie* 7, Luxembourg

FEMA-249. Assessment of the State-of-the-Art Earthquake Loss Estimation Methodologies (1994). Federal Emergency Management Agency, FEMA-249/June 1994, *Earthquake Hazard Reduction Series* 70, p. 300

Frolova, N, Larinov, V & Bonnin, J (2006). Expected damage and loss assessment in "Emergency" mode at global scale: Analysis of uncertainties. First European Conference on Earthquake Engineering and Seismology, Geneva, Switzerland, 3–8 September 2006. Paper Number: 1264

Green, RWE & Bloch, S (1971). The Ceres, South Africa, Earthquake of September 29, 1969, Part I. Report on some aftershocks. *Bulletin of the Seismological Society of America* 61, 851–9

Gutenberg, B & Richter, CF (1944). Frequency of earthquakes in California. *Bulletin of the Seismological Society of America* 34, 185–8

Gutenberg, B & Richter, CF (1956a). Magnitude and energy of earthquakes, *Annals of Geophysics* **9**(1), 1–15

Gutenberg, B & Richter, CF (1956b). Earthquake magnitude, intensity, energy, and acceleration: (Second paper). *Bulletin of the Seismological Society of America* 46, 105–45.

Haas, TN & Van der Kolf, T (2014). Seismic Analysis of URM Buildings in S.Africa. World Academy of Science, Engineering and Technology. *International Journal of Civil, Architectural, Structural and Construction Engineering* **8**(12), 1188–95

Hattingh, E, Bejaichund, M & Ramperthap, J (2006). Investigation of Ground Acceleration Attenuation Relations for Key Areas in South Africa, Council for Geoscience, Pretoria. Report no. 2006–0050

International Seismological Centre, On-line Bulletin, www.isc.ac.uk, Internatl. Seis. Cent., Thatcham, United Kingdom, 2010

Jalpa, DP & Atkinson, GM (2012). Scenario ShakeMaps for Ottawa, Canada. *Bulletin of the Seismological Society of America* **102**(2), 650–60

Jonathan, E (1996). Some aspects of seismicity in Zimbabwe and Eastern and Southern Africa. M.Sc. Thesis Institute of Solid Earth Physics, Bergen University, Bergen, Norway

Kaka, S & Atkinson, G (2004). Relationships between instrumental intensity and ground motion parameters in eastern North America. *Bulletin of the Seismological Society of America* 94, 1728–36

Keilis-Borok, VI, Kronrod, TL & Molchan, GM (1984). Seismic risk for the largest cities of the world: Intensity VIII and more. *Geneva Papers on Risk and Insurance* 9, 255–70

Keyser, AW (1974). Some macroscopic observations in the meizoseismal area of the Boland earthquake of 29th September 1969. Council for Geoscience, *Geological Survey of South Africa, Seismologic Series No. 4*, 18–25

Kijko, A (2004). Estimation of the maximum earthquake magnitude, *mmax*. *Pure and Applied Geophysics* 161, 1–27

Kijko, A (2011). Introduction to probabilistic seismic hazard analysis. *Encyclopedia of Solid Earth Geophysics*, Harsh Gupta (ed.), Springer

Kijko, A, Retief, SJP & Graham, G (2002). Seismic hazard risk assessment for Tulbagh, South Africa: Part I – Assessment of seismic hazard. *Natural Hazards* 26, 175–201

Kijko, A & Sellevoll, MA (1989). Estimation of earthquake hazard parameters from incomplete data files, Part I, Utilization of extreme and complete catalogues with different threshold magnitudes. *Bulletin of the Seismological Society of America* 79, 645–54

Kijko, A & Sellevoll, MA (1992). Estimation of earthquake hazard parameters from incomplete data files, Part II, Incorporation of magnitude heterogeneity. *Bulletin of the Seismological Society of America* 82, 120–34

Kramer, SL (1996). *Geotechnical Earthquake Engineering.* Englewood Cliffs, N.J. Prentice-Hill

Lasocki, S & Urban, P (2010). Bias, variance and computational properties of Kijko's estimators of the upper limit of magnitude distribution, *m*max. *Acta Geophysica* 59, 659–73

Lay, T & Wallace, TC (1995). *Modern Global Seismology*. London, Academic Press

Lebek, W (unpublished). Introduction to Property Commercial and Industrial Insurance and Reinsurance (Mail version). p. 53. Short course in: Continuing Education University of Pretoria, 2011

Lomnitz, C (1973). Poisson processes in earthquake studies. *Bulletin of the Seismological Society of America* 63, 735–58

McGuire, RK (2004). *Seismic Hazard and Risk Analysis.* Oakland, Earthquake Engineering Research Institute, MNO-10

Midzi, V, Bommer, JJ, Strasser, FO, Albini, P, Zulu, BS, Prasad, K & Flint, NS (2013). An intensity database for earthquakes in South Africa from 1912 to 2011. *Journal of Seismology* 17, 1183–205

Mouroux, P, Bertrand, E, Bour, M, Le Brun, B, Depinois, S, Masure, P & RISK-UE team (2004). The European RISK-UE Project: An advanced approach to earthquake risk scenarios. 13th World Conference on Earthquake Engineering Vancouver, B.C., Canada August 1–6, 2004 Paper No. 3329

Murphy, J & O'Brien, L (1977). The correlation of peak ground acceleration amplitude with seismic intensity and other physical parameters. *Bulletin of the Seismological Society of America* 67, 877–915

Neumann, F (1954). *Earthquake Intensity and Related Ground Motion*. University of Washington Press

Page, R (1968). Aftershocks and microaftershocks. *Bulletin of the Seismological Society of America* 58, 1131–68

Reiter, L (1990). *Earthquake Hazard Analysis: Issues and Insights*. New York: Columbia University Press

Reitherman, R (1985). A review of earthquake damage estimation methodologies. *Earthquake Spectra (EERI)* 1, 805–47

Richter, CF (1958). *Elementary Seismology.* Freeman WH, San Francisco

Rietbrock, A (unpublished). Stochastic GMPEs for South Africa. Presented during Thyspunt SSHAC Level 3 PSHA Close-Out Meeting, 16–18 October 2013, Kievits Kroon, Pretoria, South Africa.

Rietbrock, A, Strasser, F & Edwards, B (2013). A stochastic earthquake ground-motion prediction model for the United Kingdom. *Bulletin of the Seismological Society of America* **103**(1), 57–77

SANS 10160-4 (2009). South African National Standard. Basis of structural design and actions for buildings and industrial structures – Part 4: Seismic actions and general requirements for building. SABS Standard Division, www.sabs.co.za

Saragoni, J, Crempien, Y & Ayala, R (1982). Características experimentales de los movimientos sísmicos sudamericanos, *Revista del IDIEM* **21**(2), 67–86, México

Scherbaum, F (unpublished). Improvements in host-to-target adjustments for GMPEs in PSHA. Presented during Thyspunt SSHAC Level 3 PSHA Close-Out Meeting, 16–18 October 2013, Kievits Kroon, Pretoria, South Africa.

Shah, HC (1984). Glossary of terms for probabilistic seismic-risk and hazard analysis. *Earthquake Spectra* **1**(1), 33–40

Silva, EO, Gioacchini, G, Panella, SD, Tornello, ME & Frau, CD (2005). Relación entre aceleración del suelo e intensidad sísmica para la zona norte de la provincial de Mendoza, Argentina. Congreso Chileno de Sismología e Ingeniería Antisísmica IX Jornadas, 16–19 de Novembre de 2005, Concepción – Chile

Sobolev, GA (1997) (ed.). *Assessment of Seismic Hazard and Seismic Risk, A Handbook for Executives.* Russian Academy of Sciences. Institute Physics of Earth, Moscow

Toro, GR, Abrahamson, NA & Schneider, JF (1997). Model of strong ground motion from earthquakes in Central and Eastern North America: Best estimates and uncertainties. *Seism. Res. Lett*. 68, 41–57

Trifunac, MD & Brady, AG (1975). On the correlation of seismic intensity scales with the peaks of recorded strong ground motion. *Bulletin of the Seismological Society of America* **65**(7), 139–62

Twesigomwe, E (1997). Probabilistic seismic hazard assessment of Uganda. Ph.D. Thesis, Makarere University, Uganda

Wald, DJ, Quitoriano, V, Heaton, TH & Kanamori, H (1999). Relationship between peak ground acceleration, peak ground velocity, and modified Mercalli intensity in California. *Earthquake Spectra* **15**(3), 557–64

Whitman, RV, Reed, JW & Hong, ST (1973). Earthquake damage probability matrices. Proceedings of the Fifth World Conference on Earthquake Engineering Rome, Italy

Whitman, RV (1986). Earthquake loss estimation methodology. In *Earthquake Prognostics, Hazard Assessment, Risk Evaluation and Damage Prevention*. Proceedings from the 2nd International Seminar held in Berlin, June 24–27, 1986. A. Vogel and K. Brandes (eds.), Friedr. Vieweg & Sohn, Braunschweig/ Wiesbaden, 1986, 259–78

Wood, HO & Neumann, F (1931). Modified Mercalli Intensity Scale of 1931. *Bulletin of the Seismological Society of America* **21**(4), 277–83

APPENDIX A

DAMAGE PROBABILITY MATRICES USED

BUILDING CLASS # 3. Unreinforced masonry, bearing wall, low rise

Central damage factor (%)	Probability of damage (%) by MMI and damage state						
	VI	VII	VIII	IX	X	XI	XII
0.0	0,0	0,0	0,0	0,0	0,0	0,0	0,0
0.5	9,1	0,6	0,0	0,0	0,0	0,0	0,0
5.0	90,5	55,5	10,9	0,5	0,0	0,0	0,0
20.0	0,4	43,4	66,0	22,4	2,0	0,1	0,1
45.0	0,0	0,5	22,9	65,9	35,0	10,1	3,4
80.0	0,0	0,0	0,2	11,2	62,5	83,1	50,4
100.0	0,0	0,0	0,0	0,0	0,5	6,7	46,1

BUILDING CLASS # 8. Reinforced concrete shear wall without moment-resisting frame, medium rise

Central damage factor (%)	Probability of damage (%) by MMI and damage state						
	VI	VII	VIII	IX	X	XI	XII
0.0	2,5	0,0	0,0	0,0	0,0	0,0	0,0
0.5	59,0	8,6	0,0	0,0	0,0	0,0	0,0
5.0	38,5	89,2	66,4	11,7	0,4	0,0	0,0
20.0	0,0	2,2	33,6	83,9	56,9	19,7	3,7
45.0	0,0	0,0	0,0	4,4	42,7	77,0	77,6
80.0	0,0	0,0	0,0	0,0	0,0	3,3	18,7
100.0	0,0	0,0	0,0	0,0	0,0	0,0	0,0

BUILDING CLASS REF. # 9. Reinforced concrete shear wall without moment-resisting frame, high rise

Central damage factor (%)	Probability of damage (%) by MMI and damage state						
	VI	VII	VIII	IX	X	XI	XII
0.0	2,8	0,0	0,0	0,0	0,0	0,0	0,0
0.5	49,9	2,5	0,0	0,0	0,0	0,0	0,0
5.0	47,3	86,8	42,3	2,8	0,4	0,0	0,0
20.0	0,0	10,7	57,3	70,8	19,3	1,8	0,3
45.0	0,0	0,0	0,4	26,4	80,0	67,2	27,3
80.0	0,0	0,0	0,0	0,0	0,7	31,0	72,4
100.0	0,0	0,0	0,0	0,0	0,0	0,0	0,0

BUILDING CLASS # 6 (Green Point Stadium). Reinforced concrete shear wall with moment-resisting frame, medium rise

Central damage factor (%)	Probability of damage (%) by MMI and damage state						
	VI	VII	VIII	IX	X	XI	XII
0.0	20,4	0,0	0,0	0,0	0,0	0,0	0,0
0.5	70,3	15,5	0,0	0,0	0,0	0,0	0,0
5.0	9,3	84,5	88,4	28,9	1,4	0	0
20.0	0,0	0,0	11,6	71,1	81,6	38,7	3,8
45.0	0,0	0,0	0,0	0,0	17,0	61,3	88,7
80.0	0,0	0,0	0,0	0,0	0,0	0,0	7,5
100.0	0,0	0,0	0,0	0,0	0,0	0,0	0,0

BUILDING CLASS # 7 (Green Point Stadium). Reinforced concrete shear wall with moment-resisting frame, high rise

Central damage factor (%)	Probability of damage (%) by MMI and damage state						
	VI	VII	VIII	IX	X	XI	XII
0.0	19,1	0,0	0,0	0,0	0,0	0,0	0,0
0.5	62,9	7,2	0,2	0,0	0,0	0,0	0,0
5.0	18,0	92,2	83,4	17,6	0,6	0,0	0,0
20.0	0,0	0,6	16,4	81,9	70,1	6,2	0,7
45.0	0,0	0,0	0,0	0,5	29,3	86,5	59,2
80.0	0,0	0,0	0,0	0,0	0,0	7,3	40,1
100.0	0,0	0,0	0,0	0,0	0,0	0,0	0,0

Source: ATC-13 (op. cit.)